

6. Discussion

6.1 *Surface Evaluation for Protein and Antibody Microarrays*

In this study, the performance of eight different coatings for the generation of protein and antibody microarrays was investigated. The scope of this comparison comprised plastic as well as chemically modified glass slides that were optimised for the generation of protein and antibody microarrays. As a reference to a previous study (42) manually made poly-L-lysine slides were tested in both studies. Although the use of microarrays for the study of antibody-protein interactions as well as protein-antibody interactions have been described in several publications (37, 41, 46, 58, 66, 85), this study assessed novel microarray substrates of superior characteristics compared to microarray coatings of recent publications (42). Additionally, microarray substrates for both, antibody and protein microarray technology were, for the first time, compared simultaneously. Such a comparison is especially important, since antibodies have to maintain a native conformation of antigen binding regions to remain functional. This is in contrast to proteins, which can be denatured for common applications, such as antibody profiling. Microarray coatings that show good characteristics with regard to their use in antibody microarray technology may therefore have potential to be applied in analysis of more complex protein-protein interactions, in which native conformation of the immobilised binding partner is crucial.

The investigation of substrates for protein microarray technology (Figure 11) revealed two groups of surfaces, which displayed similar signal intensity versus spotted concentration relationships. The one with higher signal intensities comprised PEG-epoxy, epoxy, dendrimer, aminosilane as well as silanated slides. Members of the group with generally lower signal intensities were amine, poly-L-lysine activated polystyrene slides. Although FAST slides were also a member of this group, it is difficult to compare this slide, since it was scanned with a lower gain, to avoid excessive background fluorescence. Nevertheless, all tested surfaces demonstrated a saturation of mean signal intensity in the region of 2000 – 2500 amol/spot. Dendrimer coated slides showed an even earlier saturation of signal at about 940 amol/spot. This limits the dynamic range, in which a quantitative measurement in future applications may be possible, to concentrations below 2000 amol/spot.

Detection limits of all slides with respect to their use in protein microarray technology allowed a separation of all surfaces in three groups. Relatively high detection limits were

observed with amine, with detection limits of about 165 amol/spot. Relatively low detection limits were obtained with FAST slides and dendrimer slides with detection down to 63 amol/spot. All other slides display similar detection limits ranging from 94 to 110 amol/spot.

Investigation of the signal intensity versus concentration relationship for antibody microarray coatings did not reveal distinct groups as with protein microarrays. Most coatings demonstrated a linear relationship between signal intensity and concentration and only dendrimer slides displayed a saturation of signal intensity above 1880 amol/spot. Few surfaces, such as epoxy, PEG-epoxy and amine slides displayed saturation above a concentration of 3770 amol/spot.

Detection limits of antibody microarrays were, in contrast to the performance in the signal versus concentration diagram, rather diverse. A grouping of detection limits as done with protein microarrays was not possible. Activated polystyrene slides showed the highest detection limits with 1727 amol/spot, while both FAST and dendrimer slides showed the lowest detection limits with 63 amol/spot, with FAST slides showing large standard deviations. All in all, the standard deviations in this application were larger than in the protein microarray application, which points towards a more fragile system. This is expected, since nativity, as previously discussed, is a crucial feature in this application to allow the binding of the antigens.

Coefficients of variation varied between 22% and 38%. Relatively low variations were obtained with dendrimer and PEG-epoxy slides, while silanated slides display rather high coefficients of variation. Coefficients of variation of antibody microarrays were higher in comparison to protein microarrays. Only dendrimer, epoxy, FAST, and silanated slides did not show large deviations of the mean coefficient of variation between both types of applications.

In order to compare results gained in this study to results from the first evaluation described in the previous chapter, poly-L-lysine slides were tested in both. Calculations of the amount of antibodies and proteins were adjusted on recent findings, which suggest that the amount of solution transferred to the chip is 0.62 nl (34) and not 5 nl as presumed in the first evaluation (42). To maintain comparability between both studies, the same spotting machinery, protocols

and buffers were used instead of different optimised handling procedures supplied by the manufacturers. However, a different performance of poly-L-lysine slides with regard to detection limit and coefficients of variation were observed in this study. This demonstrates the difficulty of protein microarray technology to obtain identical signal intensities on repetition of experiments. Reasons for that are differing efficiencies in fluorescent labelling, as well as differences in quality between different batches of manually coated poly-L-lysine slides. This necessitates the use of identical reagents as well as the consecutive handling of different surfaces within a comparative study. Therefore, poly-L-lysine slides were evaluated in both studies to allow a relative comparison. The fact that poly-L-lysine slides, which performed quite well in the first application, did show second highest detection limits on antibody microarrays as well as relatively low signal to concentration relationship suggests that most surfaces presented in this study are superior in comparison to the previous study.

A comparison of the surface coating with regard to price displays three groups. The group with the less expensive cost per chip comprises amine, epoxy, silanated and polystyrene cell culture slides with prices of about or below 1 € FAST slides and aminosilane slides are chips in the medium price range with a price per chip of 15.4 € or 8.75 € respectively, while dendrimer slides would currently cost about 60 € (135). However, this high price is due to prototype status in which all slides are prepared manually by coating specialists. It can be foreseen that a shift to automatic production will lower the price drastically. The same holds true for the prototypes of PEG-epoxy slides, for which no price is currently available.

Although it is difficult to predict a general suitability of microarray coatings for protein and antibody microarray technology using one protein and one antibody, the results presented here point towards coatings that offer outstanding qualities in their respective area of application. As expected, one surface for both antibody and protein microarray applications could not be found. For quantitative measurements of proteins in complex samples, dendrimer slides show an excellent signal to concentration ratio. For the quantitative measurement of antibodies, PEG-epoxy slides are the surface coating of choice. For experiments that necessitate the detection of very low abundance proteins and antibodies, both, dendrimer slides as well as FAST slides are very well suited.

6.2 Multiple Spotting Technique

6.2.1 Optimisation of Production Parameters

6.2.1.1 Pin Coefficients

The introduction of pin coefficients is an easy and robust method to avoid deviations of the signal intensities. The potential sources of the deviations are manifold and include potential variation in size of the pin tip and the length of the pin. Other potential factors include deviations due to changes in the position of the robotic head and the calculation of spot intensity.

According to Genetix Ltd., the manufacturer of the pins used, the maximum error of the pin tip size is $\pm 5 \mu\text{m}$ for new 100- as well as 150-micron pins, which corresponds to deviations of up to 10.25% in spot area. Analysis of the spot diameters after scanning revealed spot diameters of $225 \mu\text{m} \pm 20 \mu\text{m}$ for 150-micron pins, which correspond to potential deviations in spot area of 18.56%. Similar deviations were observed with 100-micron pins. Although these errors can increase due to abrasion during use, these deviations should only be a minor source of error, since for the calculation of spot intensities was performed using the latest version of GenePix Pro 4.1. This software uses the arithmetic mean of the raw pixel intensities from each spot and not the sum of the pixel intensities, which causes the spot intensities to be independent of spot diameter (136) and hence eliminates the spot diameter as a source of variation. However, different mass transfers due to the length of the pins or changes in the position of the robotic head after assembly, which holds the pins in position, might be a factor of deviations. A personal analysis of the distance between the tip of the pin and the surface revealed changes of at least $50 \mu\text{m}$ between pins, with a trend of decreasing distance from pins in the right column of the head to left pins in the left column. Nevertheless, this tendency could not be confirmed in a spatial comparison with the pin coefficients.

However, deviations in the distance between pin tip and surface change the contact time of the pin tips on the chips and might therefore contribute to different mass transfers and hence signal intensities. In further experiments of Chapter 5.1 and 5.2.2.1, the obtained signal intensities were corrected by corresponding pin coefficients to reduce the effects of external factors on the results.

6.2.1.2 Immunosorbent Assay

The provision of optimal parameters for the novel application of MIST is a crucial feature. One of the most important aspects for optimisation is the preparation of a suitable buffer for

the sample to be incubated on the immobilised binder. Demands for such a buffer comprise the ability to maintain structure and function of all its ingredients, the provision of an optimal environment for specific binding onto the immobilised binder and the balancing of effects caused by the mechanical stress of spotting on blocked surface. Besides, it should not contribute to the formation of background fluorescence, it should be inexpensive, easy to handle and it should maintain a liquid environment on the spot.

To meet all these requirements, the buffer was composed of several ingredients. PBS served as a buffer, which conserves the physiological conditions by providing an adequate ionic environment and a pH of 7.5. BSA was added to confirm the blocking of the surface, so that no background fluorescence could arise by unspecific attachment of labelled proteins on the surface. Another issue of comparison was the addition of a hygroscopic substance to maintain a liquid environment for optimal binding of the sample. All three tested substances, betaine, PEG 3350 and glycerol demonstrated their suitability to provide optimal binding conditions. Nevertheless, the MIST-buffer containing glycerol was chosen for all further applications, since it yielded spots with an even and highly reproducible spot homogeneity without any tendency to spread. Moreover, glycerol is an inexpensive and ready to use chemical, with is often already a component of protein sample buffers, since it prevents ice crystal formation upon freezing of samples.

Most interestingly, all three experiments also displayed that the liquid environment is not a crucial prerequisite for immunosorbent assays performed with MIST, since all controls without any hygroscopic substances also yielded adequate signals. This points towards the fact that a chemical equilibrium is established within the time between spotting and evaporation of the droplet from the surface. This fact is due to the limited space within the droplet, which causes the rapid establishment of a chemical equilibrium by an increased rate of mass transport as described by Fick's "Law of Diffusion":

$$q_x = -D \frac{\partial C}{\partial x}$$

with q_x = rate of mass transport in the x-direction [$\text{g}/\text{m}^2 \cdot \text{s}$]

D = diffusion coefficient, [m^2/s]

C = chemical concentration [g/m^3]

x = distance [m]

6.2.1.3 *scFv Screening Assay*

Optimisation of the production parameters for a scFv-screening assay comprised the selection of an appropriate washing buffer, the determination of an optimal concentration of proteins for spotting and the selection of an appropriate strain for expression of scFv's.

For optimisation of the washing buffer, an assay was performed in which 30 monoclonal anti-poly-ubiquitin scFv's were spotted onto immobilised poly-ubiquitin and on blocked surface. After incubation, TBS-T and TBS-TT were applied as washing buffers and a direct comparison was performed by scanning both slides with the same settings (Figure 24). Evaluation of both slides displayed improved signal-to-noise ratios after washing with TBS-TT, which allowed a clearer differentiation between positive and false-positive signals.

Determination of the minimal protein concentration for spotting was performed by immobilisation of four recombinant antigens and subsequent detection by anti-RGS-His antibodies. Although this assay was not performed with recombinant antibodies, it could serve as a model to simulate the accessibility of a single binding epitopes, such as the his-tag or the scFv-binding epitope. Binding protein and poly-ubiquitin with 6 moieties were clearly detectable at a concentration of 0.05 mg/ml, while cyclophilin A and poly-ubiquitin with 3 moieties displayed clear signals only at concentrations of 0.1 mg/ml. Reasons for this may be that the his-tag is more likely to be accessible in large proteins, such as binding protein and poly-ubiquitin with 6 moieties, since only a small proportion of those are linked to surfaces and tag is hence inaccessible. To ensure sufficient accessible binding motives for scFv's, a minimal concentration of 0.1 mg/ml of each antigen were used in further experiments for spotting.

The last parameter that was optimized was the selection of the expression strain, in which two strains, TG-1 and HB2151, were compared. TG-1 is an *amber* suppressor strain, which is able to suppress termination of an *amber* stop codon by introduction of a glutamate residue at this position. This ensures the expression of all selected clones including those in which the scFv's contain *amber* stop codons. Unfortunately, since the *amber* stop codon between the scFv and the gIII gene is also suppressed, this leads to co-expression of scFv-pIII fusions, which tends to lower the overall levels of scFv expression, even in clones where there are no *amber* stop codons in the scFv itself. To circumvent this problem, selected phage can be used to infect HB2151 (a non-suppressor strain), which is then induced to give soluble expression of antibody fragments. ScFv genes that do not contain *amber* stop codons will now yield higher

levels of soluble scFv than in TG-1, but those that contain *amber* stop codons will not produce any soluble scFv's (74, 120). Both strains apply a *pelB*-secretion system for transport into periplasm, in which disulfide bonds can be formed, which stabilise the three-dimensional structure of the scFv.

A direct comparison of both strains (Figure 26) displayed that TG-1 cells are more suitable for screening assay on microarrays than HB2151. While no signals were obtained for the scFv's selected against PDLIM1 and CALM2, which were expressed in HB2151 cells, some weak signals were obtained with scFv's expressed in TG-1. These results were confirmed by ELISA (data not shown). The most likely explanation to this problem is that the transport of scFv's into the media is facilitated in TG-1 cells, since the pIII-protein interacts with the C-terminal part of the TolA domain (137, 138), which leads to destabilisation of the outer membrane and promotes the transport of scFv into the media (139). This is different from the HB2151 cells, in which no pIII-fusion protein is expressed due to the *amber* stop. Finally, the use of TG-1 is generally more favourable than the use of HB2151, since all clones are in the TG-1 strain right after selection and the number of clones that need to be shuttled to HB2151 is dramatically decreased after screening.

6.2.1.4 Enzymatic Assays

For optimisation of enzymatic assays on microarrays, three different surface coatings were assessed. Selection of the surfaces was performed according to different binding capacities, since strongly adsorbing surfaces may compromise enzymatic activity by a decreased diffusion of the substrate and an alteration of enzyme structure by immobilisation. For comparison, poly-L-lysine displaying the highest binding capacity (122) followed by polystyrene slides with a lower binding capacity and BSA-coated epoxy slides, which should provide the lowest binding capacity were selected. All three surfaces were subjected to a horseradish peroxidase assay, which serves as a reference assay for all other enzymatic assays.

The comparison revealed that polystyrene slides provided the highest average signal intensity followed by BSA-coated epoxy-slides and poly-L-lysine slides (Figure 27). The high signal intensity of the polystyrene slides are most likely due to the low binding capacity, which does not compromise the structure of the enzymes and promotes diffusion of the substrate. Moreover, polystyrene slides are readily available and manufactured automatically, which should result in relatively low slide-to-slide deviations in comparison to manually coated BSA-epoxy-slides. Another advantage of polystyrene slides is that they are also compatible

with other enzymatic reactions, such as protease activity, which could be reduced on BSA-coated epoxy slides by digestion of BSA.

6.2.2 Application of the Multiple Spotting Technique

6.2.2.1 *Immunosorbent Assay*

The results clearly demonstrated the feasibility of this technique for high-throughput multiplex screening on a single chip. Figure 29 displays a typical saturation of signal intensity with increasing antigen concentration on the antibody array and allows quantification of 1.1 amol Cy5-labelled HSA. Figure 30 and Figure 31 show characteristic linear signal to concentration ratios on protein microarrays between immobilised antigens and monoclonal or polyclonal antibodies, respectively. On these protein microarrays, as little as 2.4 amol (~0.6 µg/ml) monoclonal anti-HSA antibodies and 400 zeptomole (~40 ng/ml) polyclonal anti-fibrinogen antibodies could be detected, which is comparable to the average detection limits of 0.34 µg/ml for antigens and 1.6 µg/ml for antibodies observed by Haab and co-workers (41). The multiplex microarray shown in Figure 32 proved specificity of the technique by concentration-dependent binding of monoclonal anti-HSA antibodies on immobilised HSA, while no unspecific binding of polyclonal anti-fibrinogen antibodies was observed. In addition to the specificity of the measurements, this investigation revealed high sensitivity and demonstrated that specific recognition of proteins by their antibodies is possible, using the multiple spotting technique. Nevertheless, Figure 28 shows that high concentrations (above 10 amol/spot) result in concentration-dependent unspecific binding. Therefore, negative controls have to be performed and their signal intensities have to be subtracted.

Application of the multiple spotting technique allows direct comparison of different analytes without deviation of the results by interchip variations. This enables more accurate comparisons, since those variations can range between 12% and 60% depending on the coating of the microarray (42). MIST consumes extremely small amounts of sample, since the volumes of spotted solution are, depending on the pins, only 0.19 nl or 0.6 nl (34). Moreover, the need for extra incubation times of the analyte is eliminated and hence, allows a more rapid screening compared to conventional microarray technology. The new technique might also permit the introduction of new methodologies to microarray science, such as screening of compounds that lose their activity upon immobilisation. This is possible by immobilisation of more stable interacting partners and the subsequent application of the labile compound by MIST. This possibility was tested by screening scFv's selected from large phage display

libraries for specific binding on their respective targets (Chapters 5.2.2.2). Moreover, MIST holds the promise to solve the problem that not all antibodies remain functional after immobilisation (42), which is a major bottleneck of antibody microarray technology. Immobilisation of the protein mixture followed by administration of antibodies or scFv's by MIST could solve this problem in some applications. Furthermore, this technique may bypass the shortcomings of complex sandwich antibody microarrays. Since a multitude of secondary antibodies in a total incubation would supersede the specific signals, MIST is able to apply the matching pair for each antigen directly without interfering with neighbouring samples. This would circumvent the problem of labelling complex solutions with defined stoichiometric ratios and allow the application of antibody microarrays for the quantitative measurement of non-labelled antigens. Additionally, combinatorial synthesis and functional screening of chemical compounds on the chip is potentially possible by multiple additions of several reagents on the same spot. An additional advantage is that MIST remains compatible with the standard techniques applied in microarray science, in which the entire array is incubated and washed.

6.2.2.2 *scFv Screening Assay*

While Figure 33 and Figure 34 demonstrate successful expression and purification of all four proteins, Figure 35 and Figure 36 display the feasibility of the new technique for the screening of recombinant antibody fragments. Moreover, the figures show comparable detection limits and an equal dynamic range of the microarray experiment in comparison to ELISA. The experimental setup also indicates the advantage of the microarray approach in comparison to ELISA. While the dynamic range of the ELISA data is dependent on incubation time, the dynamic range of the chip can be freely adjusted by the settings of laser power and photomultiplier range. This is especially important due to the diverse signal levels of the clones, which depend on the overall success of each selection. Furthermore, the microarray approach allows the scanning at different intensities to enlarge the dynamic range of scFv subsets and maintains the possibility to rescan the slide after analysis. Since incubation of weakly binding scFv's may require overnight incubation, the microarray approach is a much faster alternative due to the laser scanning procedure. Both figures also demonstrate the reliability of data from the chip assay revealing low standard deviation values.

The comparison of the protein microarrays data with the ELISA data (Figure 37) displayed that the majority of the clones lay in the top right or bottom left quadrant indicating the

general trend of increasing signal intensities on the chip with increasing signal intensities in ELISA. However, some clones, for example from the cyclophilin A selection showed high binding capacity in ELISA, but not on the chip. Reasons for this may be the less favourable environment of the chip in contrast to ELISA. ELISA provides a comparably gentle environment, in which proteins are predominantly kept in the liquid phase, while the microarray approach may destabilize the antigens by temporary air contacts and by mechanical forces, due to the second spotting step, in which the scFv's are applied by contact printing onto the immobilised protein. Moreover, the large surface to volume ratio of the droplets may influence the binding characteristics of some of the more sensitive scFv's. Nevertheless, such an additional selection according to stability as performed on the chip may be desirable, since high-affinity scFv's that will be gained from such selections, should be applicable to a large variety of applications with different demands with regard to stability. Moreover, it is important that none of the clones provided intense false positive signals in the chip experiment, which were not observed by ELISA. This congruence is obvious in the PDLIM1 selection, in which one single specific clone was identified, which is identical in both, ELISA and on the chip. This confirms the reliable screening of large sets of clones on the chip surface. Figure 37 also demonstrates the practicability of the new approach for the characterisation of recombinant antibody fragment selections of varying qualities. While the poly-ubiquitin and the cyclophilin A selections provide sets with a large proportion of highly binding fragments, the PDLIM1 and CALM2 selections yield few good binders. The quality of such selections depends on several factors, such as the diversity of the phage library or the format of target molecule. The latter can be observed in the selection of the poly-ubiquitin. While CALM2, PDLIM1 and cyclophilin A provide a monomer for selection, poly-ubiquitin consists of three ubiquitin moieties and hence increases the proportion of high-affinity binders due to high avidity. To demonstrate the applicability of the technique, diagrams, displaying the results of both techniques for the 15 best-binding clones on the chip, were generated for all selections (Figure 38). The diagrams confirm that the new technique can be used for the pre-screening of clones from selections, after which a subset of the best binders from each selection can be re-arrayed for further studies, such as the screening for specificity on a multitude of different antigens.

The reliability combined with the ease of handling and the little time requirement make the new technique excelling current solutions. It allows the easy generation of several replicates on the chip and consumes very little reagents. Moreover, the cell culture plates that were used

as source plates for the second spotting step can be used for the next step of the selection procedure, the re-arranging of the strong-binding subsets. The technique does not require the transfection of the phagemid into the highly expressing HB2151 strain, but works well with the TG-1 strain used in panning. This allows streamlining of this technique into the selection process and reduces manual interaction steps. Another advantage is the composition of the media, which includes both, glucose for the tight repression of scFv production during the early growth stage and IPTG for the induction of expression, once the glucose is metabolized. This eliminates the manual addition of small proportions of IPTG to the cell cultures and promotes automation.

6.2.2.3 Enzymatic Assays

Several enzymatic assays were conducted to investigate the possibility to analyse enzymatic reactions on microarrays. Altogether, three enzymes, alkaline phosphatase, horseradish peroxidase and β -galactosidase, were tested on a microarray with regard to inhibition of enzymatic activity and determination of the detection limit. Moreover, the detection limit of cathepsin D, as a prognostic marker in breast cancer (130), was measured, to anticipate future biomedical applications of the new technique.

All enzymes were active on microarrays. The HRP assay (Figure 39 and Figure 40) clearly demonstrated that the increase of signal intensity is depended on enzymatic action. While almost no signals arose in the inhibited reaction containing sodium azide as an inhibitor (123), medium intensity signals could be seen in the uninhibited reaction without incubation, which increased upon incubation at 37°C. Negative controls lacking the enzyme, which were performed on the same chip displayed signal intensities that were not distinguishable from background (data not shown). Figure 41 shows no significant signal intensities for the dilution row without incubation, while increasing signal intensities with increasing enzyme concentration can be observed after 2 hours of incubation with a detection limit of 0.85 zmol (~ 500 molecules). While such an activity ($6 \cdot 10^{-5}$ U/ml) is comparable to the detection sensitivity determined by the manufacturer ($1 \cdot 10^{-5}$ U/ml) (140), the absolute amounts that were detected excel current detection limits.

In the alkaline phosphatase assay (Figure 42) decreasing signal intensity with increasing concentrations of its inhibitor EDTA (124) were observed, which proves functionality of AP on the microarray. The determination of the detection limit without incubation (Figure 43) showed only minor signal intensities on the microarray. However, after incubation of the

microarray for 2 hours, strong signal intensities can be observed with a saturation of the signal with increasing enzyme concentration, which clearly demonstrated enzyme activity. Quantification of the detection limit revealed 5 zmol (~ 3000 molecules AP) without incubation and 0.06 zmol (~ 35 molecules AP) after a 2-hour incubation.

The assay of inhibition for β -galactosidase is shown in Figure 44. As anticipated, it displays decreasing signal intensities with increasing concentration of its inhibitor PETG (25 , 125, 126). The same holds true for the dilution row assay, which displayed increasing signal intensities with increasing enzyme concentration (Figure 45).

The determination of the detection limit for cathepsin D as an example of a sensitive enzyme with medical relevance is shown in Figure 46. It displays decreasing signal intensities with decreasing enzyme concentration. Moreover, an increase of signal intensity after incubation could be observed, which shifted the detection limit from 648 amol/spot (32.3 U/ml) without incubation to 464 amol/spot (23.1 U/ml) after an 1-hour incubation. These results display a 10 - 15 fold lower detection limit of the microarray-based approach in comparison to the microtiter plate (141). However, since casein is not the optimal substrate of cathepsin D and was used due to limitations of the scanner with regard to the detection of certain wavelengths, lower detection limits can be expected with an optimised fluorogenic substrate.

Although unprecedented detection limits have been observed in all enzymatic assays, an optimisation of the methodology according to enzyme and substrate may allow even lower detection limits. An important point to consider in this context is the substrate concentration, which is a limiting factor in the experiments shown above and may have influenced the results by end-product inhibition. Moreover, the use of optimised buffers or hygroscopic substance other than glycerol may enhance detection and hence provide better sensitivity. Another factor is the transfer of compounds to the chip surface. While contact printing systems provide reliable deposition of compounds with varying properties, non-contact printing systems may be more adequate in some applications, since they provide more gentle handling of the enzyme and the substrate, which would be especially beneficial for the compound onto which is dispensed.

Areas of application for the enzymatic assay on the chip include the characterisation of enzymes with regard to substrate specificity or activity. This approach is especially useful in

metagenomics, which is currently seeking new enzymes with novel functionalities (142). Moreover, assays can be performed in large scale to screen for potent inhibitors or new substrates.

Another valuable application is the amplification of enzymatic reactions using enzyme-antibody conjugates. Since the development of an amplification method for proteins comparable to PCR is not in sight, the screening of complex protein samples on microarrays requires a very sensitive detection procedure current microarray technologies cannot deliver. As a first step towards enzymatic amplification of the signal, as commonly applied in ELISA, the quantification of anti-HSA molecules was performed (Figure 47). This comparison revealed a shift of dynamic range of three orders of magnitude after 3 hours of incubation in comparison to the direct label. In parallel the detection limit shifted from 55.600 molecules with the direct label to 822 molecules after enzymatic amplification for 3 hours, while an extended incubation period overnight showed decay of the fluorescent signals.

Besides fluorescent detection, chemiluminescent detection may be beneficial in some applications, which suffer from high background fluorescence or require a more sensitive detection (143, 144). This approach could be especially beneficial in drug and disease screening assays and the optimisation screening of mutants in biotechnology, both areas in which high-throughput is required.

6.3 Fibrinogenolysis Assay by Substrate Capture

Although the inhibitor assay did not yield work, even under prescribed conditions in an eppendorf tube, the results of the microarray analysis (Figure 48 and Figure 49) clearly hint towards an enzymatic attachment of Cy3-labelled fibrinogen onto immobilised fibrinogen. A non-specific attachment and clot formation of Cy3-labelled fibrinogen can be excluded, since no signals were obtained on locations onto which HSA and GAPDH were immobilised. A specific attachment of Cy3-fibrinogen onto immobilised fibrinogen without enzymatic action is unlikely due to two reasons. The first is that Cy3-labelled fibrinogen demonstrated a lack of clot formation at 4°C over a period of several months (data not shown), while non-labelled fibrinogen showed aggregation at 4°C after several minutes. This hints towards a change of the clot formation properties of fibrinogen by fluorescent labelling. The second reason, which clearly weakens the hypothesis of specific non-enzymatic aggregation of Cy3-labelled fibrinogen onto immobilised fibrinogen is the clear signal difference, which was obtained by

omitting the thrombin incubation step. Although the chip was also incubated with Cy3-labelled fibrinogen, which can be seen by the signals obtained from the anti-fibrinogen antibodies, only very low signal intensities were observed. Those signals quantify the effect of specific non-enzymatic aggregation and show the difference in signal intensity in comparison to enzymatic crosslinking. The fact that no decrease in signal intensity can be seen within the dilution row of immobilised fibrinogen is can be due to the fact that recently crosslinked fibrinogen can act as a basis for further fibrinogen attachment. This causes the signal intensities not being dependent on the initial amount of fibrinogen. Another observation that could have an effect on the signal intensities within the dilution rows of fibrinogen was observed by Wu and Diamond (145), who experienced quenching due to the close proximity of fluorophores. Due to the close assembly of Cy3-labelled fibrinogen within the fibrin clot, such quenching can have effects on the measured signal intensities.

Reasons for the failure of an inhibitor assay can be manifold. The most probable reason for the lacking inhibition of ZPPD on-chip was, that the inhibitor was washed away during the blocking step. However, the lacking ability of ZPPD and a protease inhibitor cocktail to prevent clot formation in a test tube points towards a general inhibition problem and not to an effect caused by the transfer of the assay to the chip.

6.4 Protein Expression and Analysis in Nanowell Arrays

Figure 53 shows the spectrum of cell-free expressed GFP with an emission maxima at 474 nm for both dilutions and a local maxima at 502 nm for the 1:10 dilution. The spectrum of cell-free expressed β -galactosidase was recorded after addition of the fluorogenic substrate FDG and yielded a local emission maximum at 474 nm and an overall maxima at 512 nm (Figure 54).

Both maxima at 474 nm do not display fluorescence, since they lack the Stokes shift between excitation and emission wavelength. More likely, they are the result of light scattering through particles in the transcription and translation mix, since the assembly of the measurement device (Figure 61) is prone to laser beam scattering.

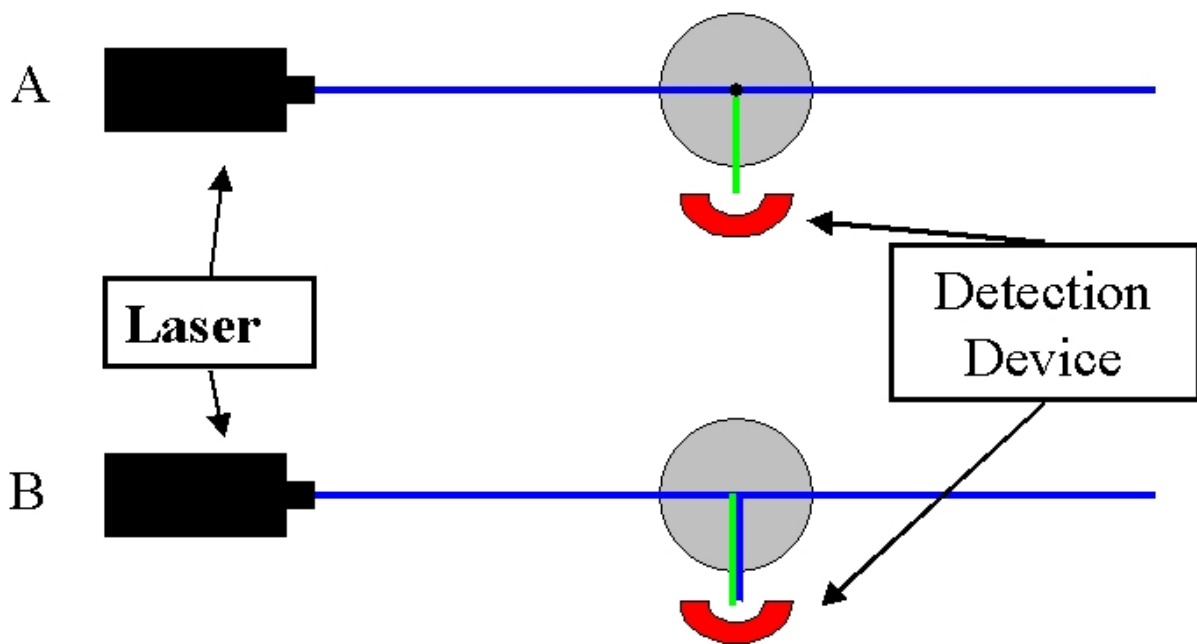


Figure 61: Principle of the fluorescence spectrometer. A displays the case for the measurement of fluorescence and B displays the scattering of the laser beam by particles in the solution

In case A the laser beam excites fluorophores and their emission is measured. However, in particular solutions, as shown in B, the laser beam can be reflected by particles, which cause an emission signal around 474 nm. This case can be seen in varying intensities in all recorded emission spectra. However, very strong intensities were seen in the 1:10 dilution of GFP, which contains large amounts of particles from the cell-free transcription and translation mix (Figure 53). A solution to this problem is centrifugation or dilution of the mix as done in the 1:100 dilution of cell-free expressed GFP, which shows a lower emission signal at 474 nm. Nevertheless, also the GFP concentration is decreased on dilution, which caused the vanishing of the typical emission peak at 509 nm (146) from the 1:10 to the 1:100 dilution step. Since the cell-free transcription and translation mix containing β -galactosidase was diluted 1:10000, the emission spectrum of β -galactosidase displayed only little emission signals at 474 nm (Figure 54). However, a clear emission signal was observed at 513 nm, which is typical for the spectrum of fluorescein.

GFP was also produced in batch and dilutions of the mix were prepared after expression. The samples were transferred to the nanowell chip to determine the detection limit in the nanowell chip (Figure 55). In parallel, a batch of transcription and translation mix was diluted 1:10 and 1:100 in PBS prior to expression to check the possibility of diluting the cell-free transcription and translation mix. After expression, different volumes of prediluted mix were

also transferred to the nanowell chip (Figure 56). All volumes, with the exception of the 720 nl volume of the 1:100 prediluted mix, displayed an increase of signal intensity with increasing volume. A quantification of the signal was possible down to a volume of 180 nl for the prediluted dilutions (Figure 56). For the mix containing GFP that was expressed undiluted, the 1:10 dilution displayed decreasing signal intensities with decreasing volumes (Figure 55), whereas no fluorescence was detected in the 1:100 dilution.

As done for GFP, dilutions of β -galactosidase from batch expression were prepared to determine the detection limit. The different samples were dispensed in volumes ranging from 180 - 720 nl into nanowells, onto predispensed substrate FDG (Figure 57). Cell-free expressed β -galactosidase was detected successfully down to a volume of 180 nl of a 1:1000 dilution with increasing signal intensities with increasing volume from 180 nl to 720 nl.

To evaluate the possibility to express GFP and β -galactosidase in nanowells, two batches of transcription and translation mix were prepared for each protein, one with and one without DNA. After expression, FDG was added to the wells in which β -galactosidase should have been produced and the nanowell chip was scanned. Diagrams of signal intensity versus dispensed volume for both batches, with and without DNA, were drawn for GFP (Figure 58) and β -galactosidase (Figure 59). Both diagrams display decreasing signal intensities with decreasing volumes as well as significant differences between the batch containing DNA and the batch without DNA. Moreover, detection of the signals down to 100 nl was possible in both cases.

The results show the feasibility of cell-free protein expression in a small-volume scale. The predilution of the translation mix is possible, since low amounts of expressed protein are sufficient for highly sensitive detection at nanolitre scale. Moreover, predilution has the further advantage of reducing the required amounts of transcription and translation mix, which reduces costs. An additional advantage is that dilution solves the incompatibility of many piezoelectric dispensers with highly viscous fluids by the significant increase of fluidity by PBS.

To address the issue that other reactions might require the addition of further compounds or solutions, a cell-free expression of GFP and β -galactosidase was performed directly in nanowells without an overlay of mineral oil using a hybridization chamber equipped with

water reservoirs. This provides a high humidity within the closed systems and enables us to reduce evaporation of samples, resulting in successfully expressed GFP and β -galactosidase directly in nanowells (data not shown).

To anticipate the use of nanowell for enzyme inhibitor screening, an assay of inhibition for cell-free expressed β -galactosidase was performed within nanowells (Figure 60). Strong inhibition of β -galactosidase activity was achieved with PETG final concentration of 1% (v/v) to 0.1% (v/v), whereas a final concentration of 0.001% (v/v) PETG resulted in comparable β -galactosidase activity levels as the non-inhibited reaction. The increase of signal intensity with decreasing inhibitor concentration reflects the inhibition of β -galactosidase activity by PETG with an IC_{50} of 3.1 μ M.

This pilot study demonstrates the feasibility to perform cell-free protein expression and characterisation in nanowell plates down to volumes of 100 nl. The format reduces the consumption of reagents required and allows the screening of large sets of samples. Moreover, screening against large protein expression libraries can be performed at reasonable cost, since consumption of cell-free transcription and translation reagents is reduced by a factor of 500. The dispensation of the reagents into nanowells can be automated, which improves accuracy and efficiency of the system. The application of cell-free coupled transcription and translation systems allows expression of toxic proteins and enhances yields for the expression of poorly expressible or insoluble proteins.